This is the accepted manuscript made available via CHORUS. The article has been published as:

Jamming in systems with quenched disorder

C. J. Olson Reichhardt, E. Groopman, Z. Nussinov, and C. Reichhardt

Phys. Rev. E **86**, 061301 — Published 3 December 2012
DOI: 10.1103/PhysRevE.86.061301

Jamming in Systems With Quenched Disorder

C.J. Olson Reichhardt[1], E. Groopman[1,2], Z. Nussinov[2], and C. Reichhardt[1]
[1] *Theoretical Division, Los Alamos National Laboratory, Los Alamos, New Mexico 87545, USA*
[2] *Department of Physics, Washington University, St. Louis, Missouri 63160, USA*

We numerically study the effect of adding quenched disorder in the form of randomly placed pinning sites on jamming transitions in a disk packing that jams at a well defined point J in the clean limit. Quenched disorder decreases the jamming density and introduces a depinning threshold. The onset of a finite threshold coincides with point J at the lowest pinning densities, but for higher pinning densities there is always a finite depinning threshold even well below jamming. We find that proximity to point J strongly affects the transport curves and noise fluctuations, and observe a change from plastic behavior below jamming, where the system is highly heterogeneous, to elastic depinning above jamming. Many of the general features we find are related to other systems containing quenched disorder, including the peak effect observed in vortex systems.

PACS numbers: 64.60.Ht,83.60.Bc,83.80.Fg,74.25.Wx

I. INTRODUCTION

When a collection of particles such as grains is at low densities with little grain-grain contact, the system acts like a liquid in response to an external drive. At higher densities, however, significant grain-grain contacts occur and the system responds like a rigid solid, exhibiting a jamming transition where the grains become stuck and develop a finite resistance to shear[1–3]. The jamming density is termed point J in simple systems such as bidisperse disk assemblies[1,3–5]. An already jammed system can be unjammed by shear[6–9] and numerous studies have focused on understanding jamming for varied grain shapes[10], interactions[11], temperatures[12], and external drives[13,14]. Depinning is another example of a transition from a stuck or pinned state to a flowing state under an applied drive, and occurs for collectively interacting particles in quenched disorder such as vortices in type-II superconductors[15–17], colloids interacting with random or periodic substrates[18–20], and charge-density waves[21]. Above depinning, the particles pass from a stationary solid state into either a moving solid or a fluctuating, liquidlike state[15,17,18]. Understanding how quenched disorder affects jamming and how jamming-unjamming transitions are related to depinning would have a great impact in both fields.

The first proposed jamming phase diagram for loose particle assemblies had three axes: inverse density, load, and temperature[1]. Here we propose that quenched disorder can form a fourth axis of the jamming phase diagram, and show that if a system has a well defined jamming transition in the absence of quenched disorder, proximity to point J is relevant even for strong quenched disorder. Jammed or pinned states below point J show profoundly different behaviors in response to an external drive compared to states above point J. We find that for varied amounts of disorder, this system exhibits many features found in vortex matter[15,22,23] including a peak effect near point J, suggesting that jamming may be a useful way to understand many of the phenomena found in systems with pinning. We study a two-dimensional (2D) bidisperse disk system with a radius ratio of $1:1.4$ that is known to exhibit jamming at a well defined density $\phi_J \approx 0.844$[4,7,13,24] for zero temperature and load. Since point J in this system is well defined in the absence of quenched disorder, we can determine how jamming changes when we add a small amount of quenched disorder in the form of randomly placed pinning sites. We focus on distinguishing the effect of jamming from that of depinning. This is particularly important since even non-interacting particles that do not exhibit a jamming transition in the absence of quenched disorder can have a finite depinning threshold in the presence of disorder.

II. SIMULATION

We consider a 2D system of size $L \times L$ with periodic boundary conditions in the x and y-directions containing N disks interacting via a short range repulsive spring force. The sample is a 50:50 mixture of disks with radii r_A and r_B, where $r_A = 1.4r_B$, and contains $N_J = 2612$ disks at ϕ_J. To initialize the system, we put down nonoverlapping disks, shrink all disks, add a few additional disks, and reexpand all disks under thermal agitation until reaching the desired density. We employ overdamped dynamics where the equation of motion for disk i located at $\mathbf{R}_i$ is

$$\eta\frac{d\mathbf{R}_i}{dt} = \sum_{i\neq j} k(R^{ij}_{\rm eff} - |\mathbf{r}_{ij}|)\Theta(R^{ij}_{\rm eff} - |\mathbf{r}_{ij}|)\hat{\mathbf{r}}_{ij} + \mathbf{F}^i_p + \mathbf{F}_D. \tag{1}$$

Here the damping constant $\eta = 1$, $k = 200$, $\mathbf{r}_{ij} = \mathbf{R}_i - \mathbf{R}_j$, $\hat{\mathbf{r}}_{ij} = \mathbf{r}_{ij}/|\mathbf{r}_{ij}|$, and $R^{ij}_{eff} = r_i + r_j$, where $r_{i(j)}$ is the radius of disk $i(j)$. The driving force $\mathbf{F}_D = F_D\hat{\mathbf{x}}$ is applied to all disks uniformly. The pinning force $\mathbf{F}^i_p$ is modeled as arising from N_p non-overlapping attractive parabolic traps with maximum force F_p and cutoff radius $r_A/2$ such that each pin can trap at most one grain. In the absence of other grains, an isolated grain depins when $F_D > F_p$. To determine if the system is pinned, we mea-

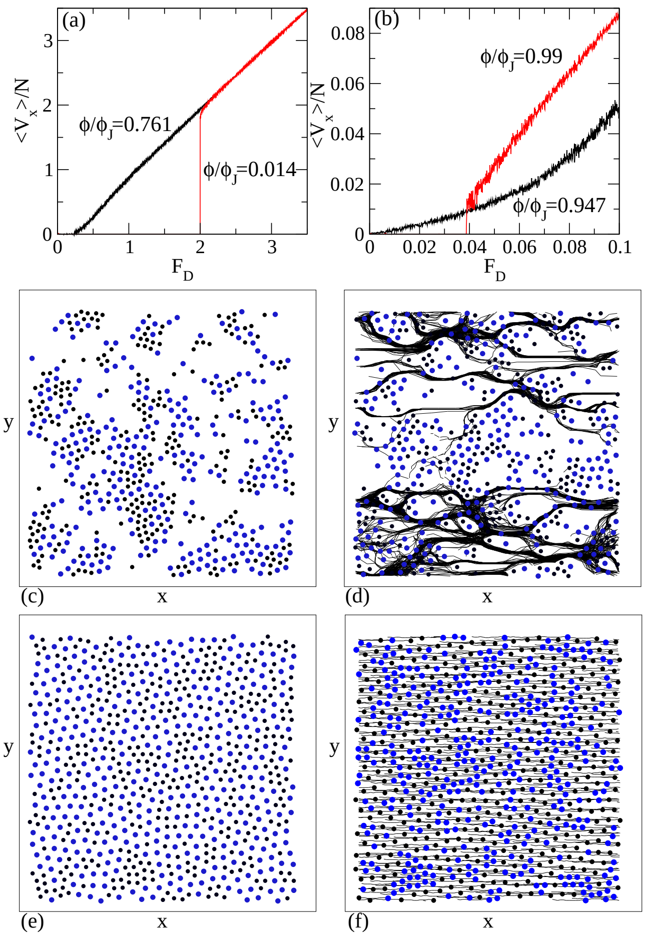

FIG. 1: (Color online) (a,b) $\langle V_x \rangle/N$ vs driving force F_D in samples with pinning strength $F_p = 2.0$. (a) Samples with pin density $N_p/N_J = 0.415$. Right (red) curve: at disk density $\phi/\phi_J = 0.014$, the critical depinning force $F_c = 2.0$. Left (black) curve: at $\phi/\phi_J = 0.761$, F_c is much lower. (b) Samples with pin density $N_p/N_J = 0.09267$. Lower (black) curve: at $\phi/\phi_J = 0.947$, $F_c = 0$. Upper (red) curve: at $\phi/\phi_J = 0.99$, F_c is finite. (c) Disk positions in the pinned state for the system with $N_p/N_J = 0.415$ and $\phi/\phi_J = 0.761$ in panel (a). (d) Disk trajectories over a period of time for the system in (c) at $F_D = 0.25 \approx 1.09F_c$ showing plastic flow above the depinning threshold. (e) Disk positions in the pinned state for a system with $N_p/N_J = 0.415$ and $\phi/\phi_J = 1.03878$. (f) Disk trajectories over a period of time for the system in (e) at $F_D = 1.1F_c$ showing elastic flow.

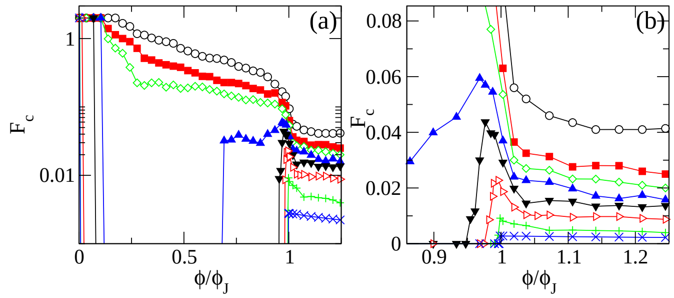

FIG. 2: (Color online) F_c vs ϕ/ϕ_J for $N_p/N_J = 0.828$ (black $\bigcirc$), 0.415 (red $\blacksquare$), 0.277 (green $\Diamond$), 0.138 (blue $\blacktriangle$), 0.09267 (black $\blacktriangledown$), 0.0346 (red $\triangleright$), 0.00692 (green $+$), and 0.00138 (blue $\times$). (a) Log-linear plot. Curves with $N_p/N_J \geq 0.277$ have $F_c > 0$ for all ϕ/ϕ_J while curves with $N_p/N_J \leq 0.138$ have a pinned regime at low ϕ/ϕ_J and another regime of finite F_c at high ϕ/ϕ_J where jamming occurs. (b) Blowup of the region near $\phi/\phi_J = 1.0$. At jamming, F_c drops for higher pinning densities and peaks for lower pinning densities.

sure the total average grain velocity $\langle V_x \rangle = \sum_{i=1}^{N} \mathbf{v}_i \cdot \hat{\mathbf{x}}$ versus F_D, where $\mathbf{v}_i$ is the velocity of grain i. We slowly increase F_D in increments of $\delta F_D = 5 \times 10^{-6}$ and wait 5×10^4 simulation time steps after each increment to ensure that the system reaches a steady state response.

III. RESULTS

In Fig. 1(a) we plot $\langle V_x \rangle/N$ versus F_D for different pin and disk densities, measured in terms of N_J and ϕ_J, respectively. At $N_p/N_J = 0.415$ and $\phi/\phi_J = 0.014$ in Fig. 1(a), the system is pinned up to $F_D = 2.0$. At this low disk density, the disks do not interact and the depinning threshold F_c is solely determined by the pinning force. For the same pinning density at $\phi/\phi_J = 0.761$, Fig. 1(a) shows that there is still a finite depinning threshold of $F_c = 0.23$ even though $N > N_p$ and there are more disks than pins. Since there are not enough pins to capture all of the disks, F_c can only be finite if the disks trapped by pins are blocking the flow of the disks that are not in pins. Thus, in pinned states such as that in Fig. 1(c), some jamming must be occurring. These heterogeneous states depin plastically, as illustrated in Fig. 1(d). Here, certain disks are always pinned while rivers of disks flow around them.

When the pinning density is reduced, F_c can vanish, as shown in Fig. 1(b) for a sample with $N_p/N_J = 0.09267$ and $\phi/\phi_J = 0.947$. Here $F_c = 0$ and the velocity response is nonlinear. As ϕ/ϕ_J decreases, F_c remains zero until N drops below N_p, when all the disks can be trapped and $F_c = F_p$. F_c is also finite at high disk densities such as $\phi/\phi_J = 0.99$ in Fig. 1(b). Below jamming in samples with small N_p/N_J, only some of the disks are immobilized, so the depinning is plastic. In the solidlike jammed state, a small number of pins can trap all the disks. Depinning is elastic above jamming, where all the disks begin to move simultaneously at the same velocity with only small localized disk rearrangements, as illustrated for $\phi/\phi_J = 1.03878$ in Fig. 1(e,f). Figure 1(b) also shows an interesting crossing of the velocity-force curves, caused by the sudden jump in $\langle V_x \rangle/N$ at depinning for the $\phi/\phi_J = 0.99$ sample.

Figure 2(a) shows the critical depinning force F_c versus ϕ/ϕ_J for different values of N_p/N_J, and Fig. 2(b) shows a blowup of the same data near $\phi/\phi_J = 1.0$. The curves with $N_p/N_J \geq 0.277$ have a finite depinning force over the full range of ϕ/ϕ_J. For the curves with

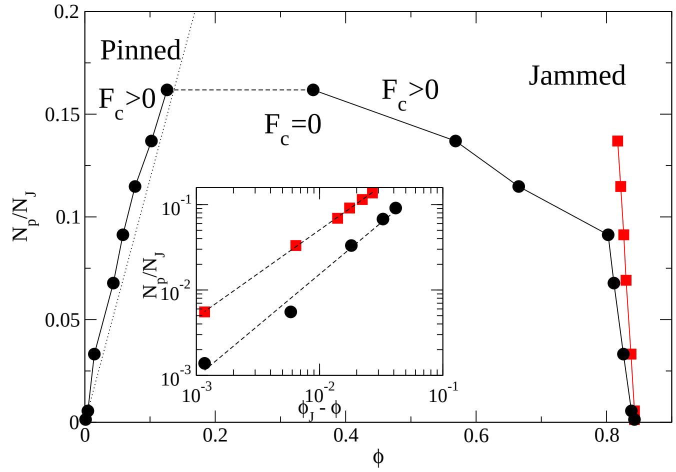

FIG. 3: (Color online) Black circles: the value of N_p/N_J at which a finite F_c first appears vs ϕ. For small ϕ, all disks are directly pinned in pinning sites, while for ϕ near $\phi_J = 0.844$, the disks are pinned due to jamming. Dotted line: $N = N_p$. Dashed line: the highest measured value of N_p/N_J at which an $F_c = 0$ region still appears. Red squares: the value of N_p/N_J at which F_c reaches its peak value vs ϕ, marking the onset of elastic depinning. Inset: the data in the main panel plotted against $\phi_J - \phi$ on a log-log scale in the region near ϕ_J. Upper dashed line: a fit with a scaling exponent of $2\nu = 1.0$; lower dashed line: a fit with $2\nu = 1.2$.

$N_p/N_J \leq 0.138$, the depinning force takes its maximum possible value of $F_c = F_p = 2.0$ at low ϕ/ϕ_J when all the disks can be trapped by pins, but for intermediate ϕ/ϕ_J, $F_c = 0$. At higher ϕ/ϕ_J, F_c becomes finite again and the system undergoes plastic depinning. In this regime, F_c increases with increasing ϕ/ϕ_J before peaking near $\phi/\phi_J = 1.0$ when the system jams. At jamming, it is possible for a single pinning site to pin the entire granular packing; nevertheless, we find that F_c at jamming decreases as N_p/N_J decreases. The depinning is elastic at and above jamming, and F_c drops with increasing ϕ/ϕ_J in this regime due to the increasing stiffness of the jammed solid.

To construct the quenched disorder-disk density plane of the jamming phase diagram, we use velocity force curves to identify the onset of a finite F_c as a function of disk density ϕ for different values of N_p/N_J. We also determine the value of ϕ at which F_c reaches its peak value near ϕ_J. In Fig. 3, the area above the data points is the region of finite F_c where pinning and/or jamming occurs. For low ϕ, when $F_c > 0$ the disks are directly pinned at pinning sites, while at high ϕ, $F_c > 0$ when the grains become jammed. The dashed line in Fig. 3 indicates the highest measured value of N_p/N_J where an $F_c = 0$ region still appears. Near this line, stochastic clogging behavior occurs that is quite distinct from the pinning and jamming transitions; this clogging will be described in[25]. The onset of a finite F_c at low ϕ falls slightly to the left of the dotted $N = N_p$ line due to the effective screening of a few unoccupied pinning sites by "upstream" occupied pinning sites that prevent disks from reaching the empty pins. Near ϕ_J we find that the quenched disorder density N_p/N_J can be considered as a new axis of the jamming phase diagram, and that the jamming density decreases with increasing N_p/N_J. The onset of jamming can be defined to occur either when F_c becomes finite or when F_c reaches its peak value at the transition from plastic to elastic depinning. Figure 3 shows that these two definitions are not identical but track each other closely near ϕ_J. The onset of elastic depinning continues to produce a peak in F_c up to the highest pinning densities we have considered.

We can make a simple argument for how quenched disorder reduces the jamming density. The average distance between pins is $l_p \propto \rho_p^{-1/2}$, where $\rho_p = N_p/L^2$. To estimate a correlation length ξ, we assume that ξ grows near jamming according to $\xi \propto (\phi_J - \phi)^{-\nu}$. Jamming should occur when $l_p = \xi$, or when $\rho_p \propto (\phi_J - \phi)^{2\nu}$. As shown in the inset of Fig. 3, a fit of the onset of finite F_c for $\phi > 0.8$ or a fit to the peak value of F_c give linear or nearly linear dependencies on ϕ (with exponents of 1.0 and 1.2, respectively), implying that $\nu \approx 0.5$. This value is close to some theoretical predictions[26], suggesting that quenched disorder shifts but does not destroy the jamming transition, and supporting the inclusion of quenched disorder as a fourth axis on the jamming phase diagram. Caution must be taken in comparing our exponent to systems without quenched disorder, since the presence of quenched disorder or the fact that we are driving our system could fundamentally change the nature of the jamming, and additional corrections to scaling could be relevant[27]. We note that the actual value of F_c in regions where a finite depinning threshold is present is not expected to exhibit critical scaling since it is an inherently nonequilibrium quantity. Near but below ϕ/ϕ_J, Fig. 4(e) shows that the shapes of the F_c vs ϕ curves vary strongly with pinning density so that no scaling is possible. Above ϕ/ϕ_J, we find $F_c \propto (N_p/N_J)^{-\gamma}$ with $\gamma \approx 0.5$. This behavior persists well above ϕ/ϕ_J and represents ordinary, rather than critical, scaling of F_c with N_p similar to that found for the depinning of superconducting vortices, where $\gamma = 1$.

The onset of jamming can also be detected by analyzing the velocity noise fluctuations using the power spectrum $S(f)$ obtained from the time series of the average disk velocities, $S(f) = |\int \exp(-i2\pi ft)\langle V_x\rangle(t)dt|^2$, at $F_D = 1.1F_c$, and the integrated noise power S_0 in the lowest spectrum octave. Figure 4(a) shows S_0 versus ϕ for $N_p/N_J = 0.277$ and Fig. 4(b) shows the same quantity for $N_p/N_J = 0.0346$. For $N_p/N_J = 0.277$ in Fig. 4(a), S_0 is low for $\phi/\phi_J < 0.3$ since there are very few collective interactions that can produce low frequency noise. For $\phi/\phi_J > 0.95$, S_0 decreases rapidly with increasing ϕ/ϕ_J after the system jams and transitions to elastic depinning. At intermediate ϕ/ϕ_J when the depinning is plastic, large velocity fluctuations occur and produce a broad band noise signal, as shown in Fig. 4(c) for $\phi/\phi_J = 0.968$. The solid line in Fig. 4(c) is a fit to $1/f^{0.9}$. The ap-

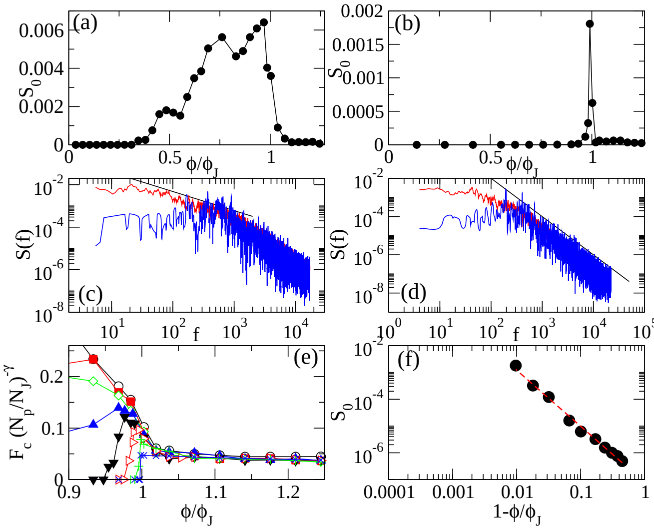

FIG. 4: (Color online) (a,b) S_0 vs ϕ/ϕ_J for $F_D = 1.1F_c$. (a) $N_p/N_J = 0.277$. S_0 drops at the onset of jamming and at low ϕ/ϕ_J. (b) $N_p/N_J = 0.0346$. S_0 peaks just below jamming. (c) $S(f)$ vs f from the system in (a) for (upper red curve) $\phi/\phi_J = 0.968$ where the depinning is plastic and (lower blue curve) $\phi/\phi_J = 1.141$ where the depinning is elastic and a narrow band noise signal appears. Solid black line: a fit to $1/f^{0.9}$. (d) $S(f)$ vs f for the system in (b) for (upper red curve) $\phi/\phi_J = 0.989$ and (lower blue curve) $\phi/\phi_J = 1.141$ showing narrow band noise in the jammed phase. Solid black line: a fit to $1/f^2$. (e) The data from Fig. 2 plotted as $F_c(N_p/N_J)^{-\gamma}$ vs ϕ/ϕ_J with $\gamma = 0.43$ for $N_p/N_J = 0.828$ (black ◯), 0.415 (red ■), 0.277 (green ◊), 0.138 (blue ▲), 0.09267 (black ▼), 0.0346 (red ▷), 0.00692 (green +), and 0.00138 (blue ×), showing noncritical scaling of F_c in the jammed region. (f) The data from Fig. 4(b) plotted as S_0 vs $1-\phi/\phi_J$ showing scaling below the jamming transition. The dotted line is a fit to $S_0 \propto (1-\phi/\phi_J)^-\beta$ with $\beta = 2.09$.

pearance of $1/f$ noise is known to be associated with plastic depinning[17,22]. For $\phi/\phi_J = 1.141$ in the elastic depinning regime, Fig. 4(c) shows that the noise power is considerably reduced and $S(f)$ has a peak at finite frequencies with several higher harmonics, indicative of a narrow band noise signal. The appearance of narrow band noise in driven systems with quenched disorder is associated with the formation of a moving solid[21,28] and is termed a washboard frequency. This is consistent with the moving jammed packing acting like a rigid solid. For the smaller pinning density of $N_p/N_J = 0.0346$, Fig. 4(b) shows a pronounced peak in S_0 at $\phi/\phi_J = 0.989$, just below the peak in F_c. On the low density side of this peak, Fig. 4(f) indicates that $S_0 \propto (1-\phi/\phi_J)^\beta$ with $\beta \approx 2$. As the system enters the jammed phase and depins elastically, S_0 rapidly drops with increasing ϕ/ϕ_J. In Fig. 4(d) we plot $S(f)$ for $\phi/\phi_J = 0.989$ and $\phi/\phi_J = 1.141$ for $N_p/N_J = 0.0346$. There is broad band noise in the plastic flow regime at $\phi/\phi_J = 0.989$ and narrow band noise in the elastic flow regime at $\phi/\phi_J = 1.141$.

IV. DISCUSSION

The depinning-jamming transition we observe has many similarities to the peak effect phenomenon that can occur as a function of vortex density in type-II superconductors with vortices moving through random disorder. At low densities, the depinning threshold F_c is high since vortices can be pinned individually. For intermediate densities, F_c remains low until, at higher density, F_c increases rapidly to a peak value and the noise power simultaneously increases dramatically[15,22,23]. The peak effect and the noise features are more prominent in cleaner samples with less pinning[23]. All these features are captured in our results. The standard interpretation of the peak effect is that it marks a transition from a weakly pinned solid to a more strongly pinned disordered state. Our results suggest that the peak effect may be a general phenomenon in other systems with quenched disorder close to some type of phase transition.

V. SUMMARY

In summary, we show how jamming behavior changes with the addition of quenched disorder using a simple model of bidisperse disks that exhibit a well defined jamming density ϕ_J in the absence of quenched disorder. We propose that quenched disorder represents a new axis of the jamming phase diagram and show that increasing the quenched disorder density decreases the disk density at which the system jams. At low disorder densities, the disk density at which a finite depinning threshold appears coincides with point J. There is also a reentrant finite depinning threshold at low disk densities when all the disks are directly pinned. We find a maximum in the depinning threshold at the onset of jamming for low disorder densities. When the disorder density is sufficiently large, the depinning threshold is finite for all disk density values; however, proximity to ϕ_J produces clear effects in the form of features in the velocity force curves as well as noise fluctuation signatures. Below jamming, the depinning is characterized by heterogeneous plastic flow and $1/f$ noise characteristics, while above jamming, the depinning is elastic with all the disks moving together and is characterized by a washboard noise. For high disorder density, jamming is associated with a drop in the depinning threshold instead of the peak in depinning found at low disorder density. Our results show many similarities to the peak effect observed in high-temperature superconductors where a depinning threshold peak occurs at both low and high vortex densities. Our results should be relevant for systems exhibiting depinning transitions and jamming.

Acknowledgments

This work was carried out under the auspices of the NNSA of the U.S. DoE at LANL under Contract No. DE-AC52-06NA25396. Z.N. was supported by NSF DMR-1106293 at WU.

[1] A.J. Liu and S.R. Nagel, Nature (London) **396**, 21 (1998).
[2] T.S. Majmudar, M. Sperl, S. Luding, and R.P. Behringer, Phys. Rev. Lett. **98**, 058001 (2007).
[3] A.J. Liu and S.R. Nagel, Annu. Rev. Condens. Matter Phys. **1**, 347 (2010).
[4] C. S. O'Hern, L.E. Silbert, A.J. Liu, and S.R. Nagel, Phys. Rev. E **68**, 011306 (2003).
[5] C. Zhao, K. Tian, and N. Xu, Phys. Rev. Lett. **106**, 125503 (2011).
[6] D. Howell, R.P. Behringer, and C. Veje, Phys. Rev. Lett. **82**, 5241 (1999).
[7] P. Olsson and S. Teitel, Phys. Rev. Lett. **99**, 178001 (2007); M. Otsuki and H. Hayakawa, Phys. Rev. E **83**, 051301 (2011); P. Olsson and S. Teitel, Phys. Rev. E **83**, 030302(R) (2011).
[8] D. Bi, J. Zhang, B. Chakraborty, and R.P. Behringer, Nature (London) **480**, 355 (2011).
[9] C. Heussinger and J.-L. Barrat, Phys. Rev. Lett. **102**, 218303 (2009); C. Heussinger, P. Chaudhuri, and J.L. Barrat, Soft Matter **6**, 3050 (2010).
[10] M. Mailman, C.F. Schreck, C.S. O'Hern, and B. Chakraborty, Phys. Rev. Lett. **102**, 255501 (2009); A. Donev, R. Connelly, F.H. Stillinger, and S. Torquato, Phys. Rev. E **75**, 051304 (2007).
[11] G. Lois, J. Blawzdziewicz, and C.S. O'Hern, Phys. Rev. Lett. **100**, 028001 (2008).
[12] Z. Zhang, N. Xu, D.T.N Chen, P. Yunker, A.M. Alsayed, K.P. Aptowicz, P. Habdas, A.J. Liu, S.R. Nagel, and A.G. Yodh, Nature (London) **459**, 230 (2009).
[13] J.A. Drocco, M.B. Hastings, C.J. Olson Reichhardt, and C. Reichhardt, Phys. Rev. Lett **95**, 088001 (2005).
[14] R. Candelier and O. Dauchot, Phys. Rev. E **81**, 011304 (2010).
[15] S. Bhattacharya and M.J. Higgins, Phys. Rev. Lett. **70**, 2617 (1993).
[16] M.C. Faleski, M.C. Marchetti, and A.A. Middleton, Phys. Rev. B **54**, 12427 (1996).
[17] C.J. Olson, C. Reichhardt, and F. Nori, Phys. Rev. Lett. **81**, 3757 (1998).
[18] C. Reichhardt and C.J. Olson, Phys. Rev. Lett. **89**, 078301 (2002).
[19] A. Pertsinidis and X.S. Ling, Phys. Rev. Lett. **100**, 028303 (2008).
[20] T. Bohlein, J. Mikhael, and C. Bechinger, Nature Mater. **11**, 126 (2012).
[21] G. Grüner, Rev. Mod. Phys. **60**, 1129 (1988).
[22] A.C. Marley, M.J. Higgins, and S. Bhattacharya, Phys. Rev. Lett. **74**, 3029 (1995).
[23] S.S. Banerjee *et al.*, Phys. Rev. B **62**, 11838 (2000).
[24] C.J. Olson Reichhardt and C. Reichhardt, Phys. Rev. E **82**, 051306 (2010).
[25] C.J. Olson Reichhardt and C. Reichhardt, to be published.
[26] M. Wyart, L.E. Silbert, S.R. Nagel and T.A. Witten, Phys. Rev. E **72**, 051306 (2005).
[27] D. Vagberg, D. Valdez-Balderas, M.A. Moore, P. Olsson, and S. Teitel, Phys. Rev. E **83**, 030303 (2011).
[28] S. Okuma and N. Kokubo, Phys. Rev. B **61**, 671 (2000).